

Electrical, Structural and Processing Properties of Electrically Conductive Adhesives

Li Li, Christine Lizzul, Hansoo Kim, Isaac Sacolick, and James E. Morris, *Senior Member, IEEE*

Abstract—There is growing interest in the potential of electrically conductive metal-loaded polymer adhesives for solder replacement in SMT and other microelectronic applications. Eight commercial electrically conductive adhesive pastes were selected for study, including both thermosetting and thermoplastic examples. All were silver based, except for one nickel-polymer composite. The properties on which this work is focused are the microstructure and electrical characteristics, with the specific purpose of determining the conduction mechanisms. The electrical measurements establish that the primary source of electrical resistance is in the silver particles, with negligible contact effects between them. Differential scanning calorimetry results indicate that drifts in the electrical properties are not attributable to incomplete cures. Electrical measurements on simplified structures prepared in the laboratory are also reported.

I. INTRODUCTION

ELECTRICALLY conductive adhesives (ECA's) of resistivities less than $10 \Omega \cdot \text{cm}$ are formed from high resistivity polymers by doping the polymer matrix with metal fillers. Two types of polymer conventionally used are thermoplastic and thermosetting, each with advantages and disadvantages. More recently developed materials are mixtures of both. If a very large amount of filler is required for conduction, the polymer material's strength and elasticity may be degraded. It is therefore important to use the minimum quantity of conductive filler to achieve the required degree of electrical performance. Percolation theory predicts a "critical" filler concentration, at which a three-dimensional network is established and conductivity increases suddenly by several orders. Thereafter, conductivity changes slowly with increase in filler concentration [1], [2].

Filler particles may come in the form of spheres, fibers, flakes or granules, but the optimum geometry is that which provides minimum critical filler concentration for low resistance, the best contact between neighboring metallic particles, and strongest adhesion to the polymer, i.e. flakes, due to their high aspect ratio [2]. Small particles are better than large, providing more particle to particle contact, greater conductivity and consistency of product [3].

ECA's are most typically filled with silver flakes. For lower cost adhesives, nickel-filled systems offer lower conductivity, and the copper-filled systems may be unstable after exposure to

high temperatures due to oxide growth on the particle surfaces. [4].

ECA composites have some immediate advantages over solder as a means of electrically conducting attachment of chip or package lead to board pad. The first is a reduction in processing steps for surface mount device manufacture from nine nominal steps using solder to only five. They also eliminate environmentally harmful lead and flux removal solvents [5].

Small thin surface-mount plastic packages experience exceptionally high stresses intensified by soldering at over 220°C . ECA's offer lower processing temperatures, reducing problems associated with solder joint fatigue and stress induced cracking, and decreasing stress on heat sensitive components. Typical ECA's cure at temperatures ranging from 80°C to 140°C , but some two component ECA's can be cured at room temperature [6]. ECA coefficients of thermal expansion are more closely matched than solder's to that of epoxy-fiberglass, and offer a more compliant attachment, minimizing failures with high flexibility, creep resistance, and stress dampening [7].

ECA silver particles around $10\text{--}20 \mu\text{m}$ in size facilitate finer line resolution than is possible with the $20\text{--}45 \mu\text{m}$ metal particles found in solder pastes. Solder paste flow after printing also restricts the line resolution, whereas ECA's have little or no flow during cure [7].

While ECA costs are roughly three times those of solder, the difference is more than offset by reduced weight use, lower capital equipment cost, and reduced numbers of production steps required to complete a soldered assembly. The epoxy technique offers quicker production throughput, due to shorter processing times and less handling of assemblies [7]–[9].

ECA drawbacks include moisture absorption and silver migration [10]. Nonselective wetting by currently available ECA materials cannot provide the same self-alignment feature as solder does. Rework is not as convenient as for solder, but is possible with various techniques. Another possible production problem (air entrapment) has been identified in this study and is discussed below.

II. ELECTRICAL PROPERTIES

The purposes of this part of the project were to determine the frequency dependence of the electrical properties, to study any nonohmic behavior, to measure the temperature coefficient of resistance (TCR), and to determine possible conduction mechanisms. All materials used in these experiments were purchased from suppliers as standard products.

Manuscript received March 1, 1993; revised July 31, 1993. This paper was presented at the 43rd Electronic Components and Technology Conference, Orlando, FL, June 1–4, 1993. The work was supported by the Integrated Electronics Engineering Center at Binghamton University.

The authors are with the Department of Electrical Engineering, Binghamton University, Binghamton, NY 13902-6000.
IEEE Log Number 9215008.

Experimental Procedures

Samples: All the specimens were prepared as 7.46 cm long 0.16 cm wide tracks in a "U" configuration on an etched FR-4 substrate. This relatively long sample length was chosen to increase sample resistances and achieve acceptable accuracy with the equipment available for rapid complex impedance measurement. Three sample thicknesses were fabricated in order to observe the dependence of electrical properties on the thickness of the adhesives. The samples which were screen printed onto the substrate have a thickness of 50 μm , while those which were made using a brass stencil have a thickness of 900 μm . Thicker stenciled samples displayed properties similar to those of the brass stenciled ones. Both sets of stenciled specimens can therefore be regarded as bulk samples, i.e., with all dimensions more than an order of magnitude greater than particulate sizes. All samples were cured according to the manufacturers' instructions.

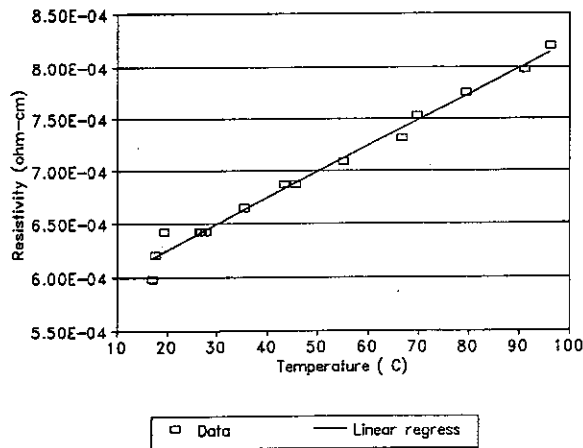
DC Resistance Measurement: The dc resistances of the samples were measured using a 4-point probe configuration and constant current sources ranging from 10 to 99 mA. The voltage probe separation was 6.65 cm.

Temperature Dependence of Bulk Resistivity: The TCR's were determined with dc source currents of 10 and 40 mA at temperatures ranging from 10 to 100°C. Representative results are shown in Fig. 1 for two Ag-filled samples. Fig. 1(a) is typical of thermoset specimens, while the thermal drift displayed in Fig. 1(b) persists in well aged thermoplastic materials.

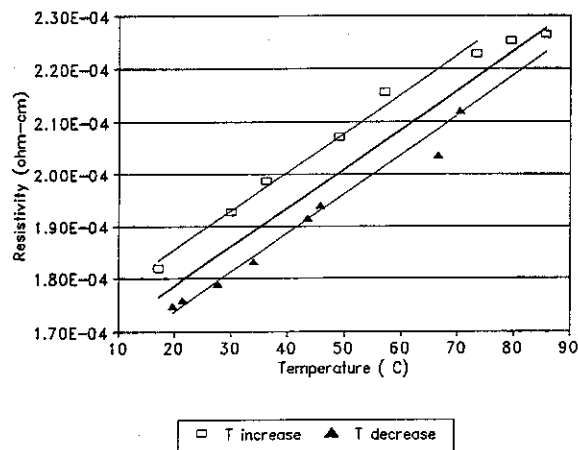
Complex Impedance: The complex impedance was measured in the frequency range of 100 Hz to 40 MHz using an HP4194A impedance/gain phase analyzer. Two test fixtures were used for measuring the impedances, the HP16047D sample holder, and a four point HP16048A test lead. A typical plot of the complex impedance versus frequency is shown in Fig. 2. The dotted lines represent a simple equivalent R - L series model simulation which is closely matched to the measurement data. The variations of the resistance and inductance with frequency so obtained for a brass stenciled Ag-filled sample are shown in Fig. 3.

III. RESULTS AND DISCUSSION

DC Resistance and Bulk Resistivity: It was expected that one would see evidence of contact resistance between particles, with various conduction mechanisms possible, such as tunneling, hopping, or bulk conduction through a semiconducting oxide phase. All of these are expected to exhibit negative or zero TCR's, (or at least less than silver's), and possibly nonohmic effects. The results of the dc resistance experiments showed that there were no observable nonohmic effects at the relatively low current densities employed. The slopes of resistivity versus temperature (e.g., Fig. 1) give TCR values ranging from 3.5 to $3.8 \times 10^{-3}/^\circ\text{C}$ for the silver-filled samples, corresponding closely to the bulk TCR for silver, reported variously as 3.8 to $4.1 \times 10^{-3}/^\circ\text{C}$ [11]. The fact that the TCR of the samples is so close to that of bulk silver (always within 10%, but usually nominally the same) indicates that ECA electrical resistance is dominated by photon scattering



(a)



(b)

Fig. 1. Resistivities for various temperatures. (a) Brass stenciled CT-5047-02 thermoset sample (TCR = 0.0039/ $^\circ\text{C}$). (b) CSM-933-65-1 screen printed thermoplastic sample (TCR = 0.0038/ $^\circ\text{C}$).

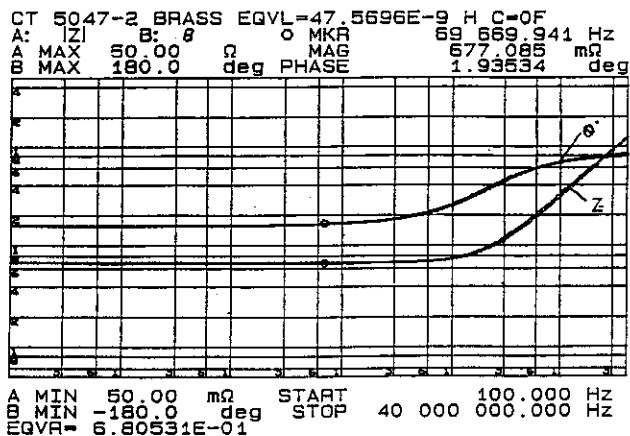


Fig. 2. Complex impedance versus frequency for a silver-filled brass-stenciled sample.

in the silver particles, with minimal (and usually negligible) contact effects between particles.

However, the resistivities of the samples are about 20–600 times the resistivity of bulk silver ($1.62 \times 10^{-6} \Omega \cdot \text{cm}$ [12]). The lower limit of this range is easily predicted by

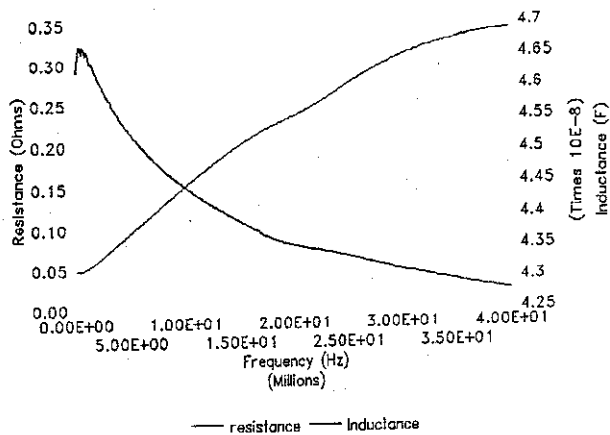


Fig. 3. Typical results of resistance and inductance versus frequency for a silver-filled brass-stenciled sample.

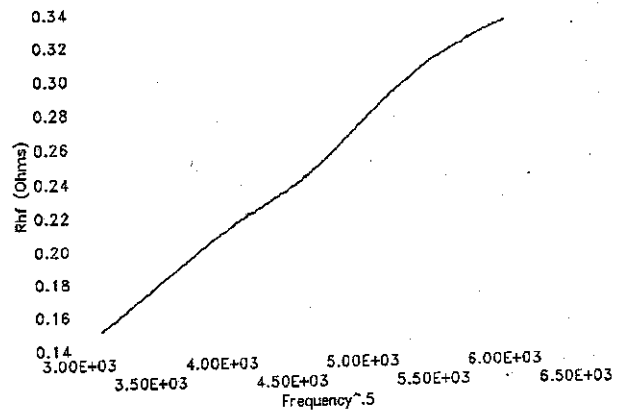


Fig. 4. This graph shows the linear relationship between the resistance at high frequencies and the square root of frequency.

the bulk silver properties and a simple structural model. If the roughly 20% volume fraction of the silver particles is equally partitioned between continuous chains running in the *x*, *y*, and *z* directions, one reaches a figure of 15 times bulk resistivity, clearly a lower limit with no disordering effects. Meandering conduction paths are the result of material disorder and imperfect particulate contacts, and raise resistivity dramatically, particularly near the percolation threshold. When any sample dimension becomes smaller, typically below about 10 times the particle size, the percolation path begins to be constrained to the other two dimensions, further increasing material resistivity. The resistivities for screen printed samples are systematically higher than for stenciled samples (although on the same order of magnitude for the relative thicknesses used here).

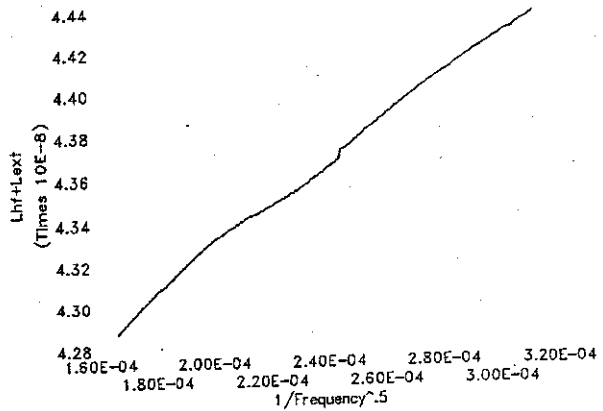


Fig. 5. This figure exhibits the linear relationship of the inductance at high frequencies with $1/\sqrt{f}$.

The samples which were filled with the smaller silver flakes demonstrated the lowest resistivity. Smaller flakes provide more particles per unit volume as anticipated above.

Frequency dependence: The frequency dependences of the resistance and inductance are shown in Fig. 3. The increase in resistance and the decrease of the inductance suggest skin effect as a possible explanation.

With direct current or alternating currents at low frequencies the inductance and resistance of a conductor are constant, based on the assumption that the current is uniformly distributed over the cross section of the conductor [13].

At higher frequencies, for good conductors, the current density no longer remains uniform, becoming concentrated at the surface of the conductor. This "skin effect" increases the effective resistance. The conductor's internal inductance, additional to any external inductance, is also affected. The skin depth δ [14] is equal to

$$\delta = \sqrt{\frac{1}{\pi \mu f \sigma}} \quad (1)$$

where f , μ , σ are the signal frequency, permeability of the medium, and conductivity of the conductor, respectively. The skin effect surface resistance, R_s per unit surface area, and reactance $X = \omega L_i$, are both frequency dependent and in general not equal [14]. At sufficiently high frequencies, when the skin depth is much smaller than the conductor's cross

section, $R_s \approx X$ [12] with

$$R_s = \omega L_i = \frac{1}{\delta \sigma} = \sqrt{\frac{\pi f \mu}{\sigma}} \quad (2)$$

and [13]

$$L_i = \frac{1}{2\pi f} \sqrt{\frac{\pi f \mu}{\sigma}} = \frac{1}{2} \sqrt{\frac{\mu}{\pi f \sigma}} \quad (3)$$

Equations (2) to (3) explain the increase in resistance and the decrease in inductance for conductive adhesives shown in Fig. 3 (for the frequency range of 10–40 MHz). The resistances show a linear dependence with the square root of frequency which is illustrated in Fig. 4 in agreement with (2).

At high frequencies the total inductance (which is equal to $L_i + L_{ext}$), explicitly demonstrates a linear correlation with $1/\sqrt{f}$ which agrees with (3), as illustrated in Fig. 5 (for the frequency range of 10–40 MHz again). Furthermore, when the internal reactance X_s is separated from the total reactance by means of this graphical technique, it agrees with the skin effect resistance R_s , as required by the theory, to within 10%.

IV. CONCLUSIONS

Measurements of the bulk ECA resistances show that nonohmic effects were not present in the adhesives. The

TABLE I
PHYSICAL AND ELECTRICAL PROPERTIES OF THE CONDUCTIVE ADHESIVES

Manufacturers	Emerson & Cuming	Emerson & Cuming	Emerson & Cuming	Emerson & Cuming	Ablestik	Tra-Con	Zymet	Transene
Materials	CSM-933-65-1	C-14-7	CT-5047-02	CS-489-02	Ablebond 16-1	Traduct 2902	SL 100-2 × 1	Nickel-Bond 60
Type	Thermoplastic	Thermoset	Thermoset	Thermoplastic	Thermoset	Thermoset	Thermoset	Thermoset
Composition	1-Component Ag	2-Component Ag & Sn	2-Component Ag	1-Component Ag & Sn	2-Component Ag	2-Component Ag	1-Component Ag	2-Component Ni
Microstructure (in diameter)	7-10 μm flakes < 1 μm flakes	10-15 μm flakes 3-15 μm spheres	5-10 μm flakes 2-3 μm flakes	10-15 μm flakes 3-15 μm spheres	10-15 μm flakes 1-5 μm flakes	3-10 μm flakes	2-4 μm flakes < 1 μm flakes	3-25 μm flakes
Resistivity (×10 ⁻⁴ Ω-cm)	1.1	18.5	6.3	8.7	6.1	9.6	3.5	100
TCR (/°C)	0.0038	0.0039	0.0039	0.0037	0.0035	0.0040	—	—

measurements of the bulk resistivities at several temperatures demonstrate that bulk silver is the primary contributor, indicative of good particle to particle contact. The expected observation of capacitive coupling between alternative conducting paths did not materialize. At high frequencies the loss due to skin effect becomes important. Current crowding on the surface of the Ag conductor increases the effective resistance of the sample which is proportional to the square root of frequency. The samples also exhibit an internal inductance L_i due to magnetic flux penetration and proportional to $1/\sqrt{f}$, in addition to the external inductance. Repeated thermal cycling demonstrated the inadequacy of quoted cure schedules to achieve stable electrical properties [15].

V. MICROSTRUCTURE

Eight commercial ECA pastes selected for this study are listed in Table I, which includes resistivity and TCR results and qualitative observations from the scanning electron microscopy studies.

Experimental Procedure

SEM samples were prepared for both surface and cross-section microstructural studies. For the surface observations, a thin layer of adhesive was prepared on a SEM sample holder. Polished cross-section samples were prepared by mechanical polishing of the cured adhesives. Fracture cross-section samples were cracked in liquid nitrogen to get a sharp fracture section. All the observations were made on an ETEC Auto Scan electron microscope.

Samples were degassed under vacuum (33 kPa) for 1 h. Some samples were made without degassing for purposes of comparison.

The compositions of samples were determined by energy dispersive spectroscopy (EDS). The EDS analysis was done on a DeltaPro Analyzer with a Super Quantum Detector and ETEC Auto Scan with a PGT System 4 Plus Analyzer.

VI. RESULTS AND DISCUSSION

The electrical and mechanical properties of the metal-loaded polymer adhesives depend on the properties of both compo-

nents (metal and polymer), as well as on the microscopic structure of the composites and on the method of preparation, e.g., vacuum, outgassing treatment, the way the sample is mixed, the matrix and its cure schedule, etc.

SEM and EDS Studies: Figs. 6(a) and (b) are two typical SEM micrographs of the conductive adhesive surfaces, selected to compare two different structures. Fig. 6(a) shows that the silver flakes in SL 100-2 × 1 fall into two distinct size ranges, 2-4 μm, and less than 1 μm. These are the smallest flake sizes seen in all the silver filled adhesives studied here. All the other flakes have a size range around 10 μm as shown in Fig. 6(b) for CS-489-02. Spherical particles also exist in this material. Another feature observed in these SEM micrographs of the ECA surfaces is that all the flakes align themselves along the surfaces. This may provide a practical advantage in tending to produce lower contact resistances. Table I lists the particles' sizes for each of the materials as estimated from the SEM investigations.

The micrographs shown in Figs. 7(a) and (b) reveal two of the mechanically polished cross-section features. Here in the cross section inside the materials, the flakes are oriented differently than on the surface. Fig. 7(a) is of a nickel-filled adhesive. The nickel flakes have a wider range of sizes than any of the other samples, ranging from 3 to 20 μm. Figure 7(b) is another sample, which also contains spherical particles, of diameters from 3 to 15 μm. In order to identify these spherical particles, EDS analyses were focused on areas of both flake and sphere. Figs. 8(a) and (b) show the EDS spectra for the flake and sphere areas, identifying the flakes as silver and the spherical particles as tin. Tin sphere fillers are added because they are cheaper than silver, and as shown in Fig. 7(b), the silver flakes align themselves around the large spheres, reducing the critical volume fraction V_c (or resistivity for a given composition) and hence the cost of the materials. This effect parallels the reduction in V_c achieved with large insulator and small conductor spherical particles in simple percolation systems [16].

Almost all the eight commercial conducting adhesives contain broad size distributions of flakes. All the flake size ranges are similar except SL 100-2 × 1, described above. Studies of the effects of size distributions on the electrical properties of conductive adhesives [17] show that formulations

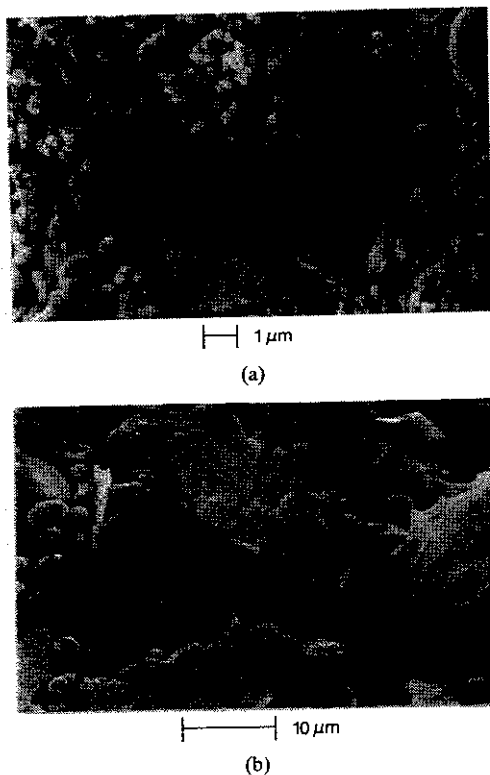


Fig. 6. Scanning electron micrographs of conducting adhesive surfaces. (a) SL 100-2 \times 1. (b) CS-489-02.

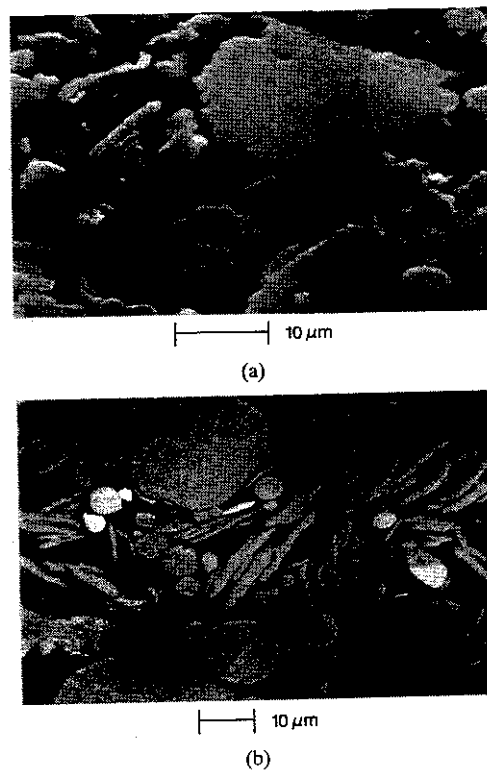


Fig. 7. Scanning electron micrographs of the polished cross-section of the conducting adhesives. (a) Nickel-bond 60. (b) C-14-7.

incorporating narrow particle size distributions require greater concentrations of particles to exceed the percolation threshold for electrical conduction than if broad particle distributions

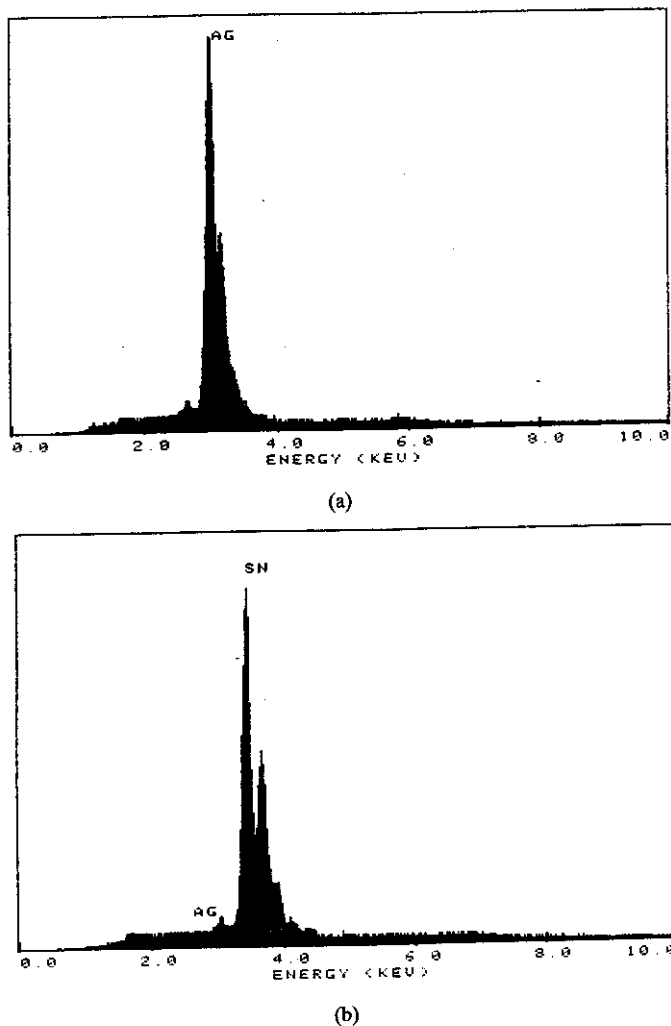


Fig. 8. Energy dispersive spectroscopy results of the selected areas. (a) C-14-7 flake. (b) C-14-7 sphere.

are used. Commercial ECA vendors all try to exceed the percolation threshold using the minimum amount of silver flakes, to both maximize adhesion and minimize cost.

Figs. 9(a) and (b) show the fracture cross sections of the samples selected. Fig. 9(a) clearly shows that bubbles remain in the sample if no degassing procedure is used. The voids will cause inferior mechanical, electrical, and thermal properties. The flakes inside the bubble are all oriented to align with the surface. Fig. 9(b) is the fracture cross section after degassing. It is shown that no air bubbles exist above a depth of about 300 μm from the surface, but that the bubbles still exist deeper. For commercial use, the thickness of the material applied will be less than 300 μm . Therefore, it will be advantageous to add a degas step in the processing procedure in order to eliminate air bubbles. If the adhesive pastes are thinned sufficiently prior to application, it is easy to remove bubbles. The degassing qualities also depend greatly on the adhesive's viscosity, on whether the adhesive contains volatile components (mainly solvents) [18], on the vacuum pressure, and on degassing times.

The composition of each specimen was analyzed by EDS. The adhesives are all silver based except Transene Nickel-bond

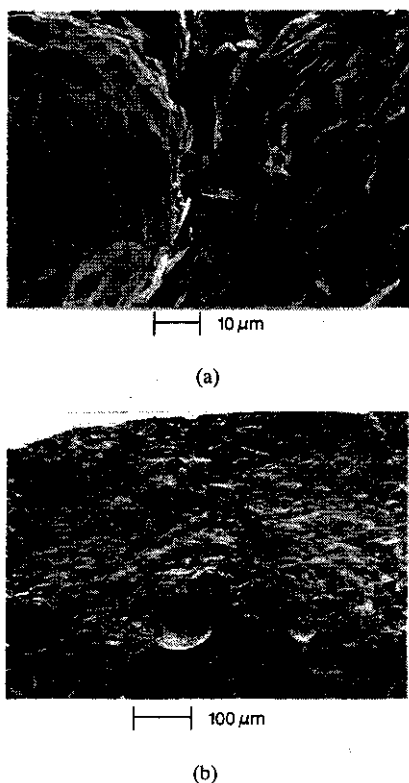


Fig. 9. Scanning electron micrographs of fracture cross-sections of the conducting adhesives. (a) CS-489-02. (b) C-14-7.

TABLE II
EDS ANALYSIS RESULTS: PERCENTAGE BY WEIGHT

Weight %	Element & Lines				
	C(K α)	O(K α)	Cl(K α)	Ag(L α)	Sn(L α)
CSM-933-65-1	21.96	0.78	0.37	76.89	—
C-14-7	17.26	2.95	0.36	69.37	10.06

60 which is filled with nickel. C-14-7 and CS-489-02 are silver filled but also contain tin spheres. The results of standardless EDS analysers (xpp quantitation) are listed in Table II. The silver weight percentage is about 76.89%, with the volume percentage of silver calculated at 22.7% from the densities of adhesive and silver. This is above the percolation threshold (about 15%) predicted by percolation theory [19].

VII. PROCESSING

Differential Scanning Calorimetry

A differential scanning calorimeter (DSC) was used to measure the heat released, starting cure temperature, and the duration of the curing process of all eight commercial ECA's, and in particular to seek evidence of multiple reactions. Peaks in the output data are interpreted as chemical reactions in the samples. An upwards peak is an endothermic reaction, usually signifying evaporation here. A downward peak is exothermic and occurs when the material is curing. A typical heating cycle consists of an initial isotherm, followed by a heating period,

TABLE III
RESULTS FROM THE DSC EXPERIMENT

	Cure Temp.	Reaction End	Heat Released
	(°C)	(°C)	(mCal)
CS-489-02	30.0	67.7	+5.76
Ablebond 16-1	67.4	110.1	-28.6
Nickel-Bond 60	74.9	100.4	-76.7
Traduct 2902	47.8	86.5	-75.8
CSM-933-65-1	50.6	85.8	+4.58
CT-5047-02	57.4	98.05	-86.9
C-14-7	64.5	111.4	-65.3
SL 100-2 \times 1	157.4	162.7	-96.3

and a final isotherm. Sample "runs" consist of multiple heating cycles.

Testing Procedures: Each conducting adhesive was cycled twice in the DSC, with heating periods and isotherms based on the data supplied by the manufacturers. The data from the first cycle shows the reaction from curing. The second cycle represents the heat capacity of the sample and is subtracted from the first. The starting temperature of each run was 30°C and the heating rate was 10°C/min. Note that the curing schedule is dependent on the size of the sample. For this experiment, samples were 4-6 mg, an amount smaller than typically used for a solder joint.

Results: Fig. 10 shows sample plots of the data. The thermosets each had an exothermic peak representing curing. The two thermoplastics showed endothermic peaks due to the evaporation of the solvent. The only anomalies to this pattern were Traduct 2902, which had both an exothermic peak followed by an endothermic peak, and Zymet SL 100-2 \times 1, which cured at a much higher temperature but much faster. Table III contains the calculated data from the experiment. The second column is the temperature where the curing or evaporation reaction began. The end of the reaction occurs at the peak of the heat released from the reaction.

VIII. CONCLUSIONS

DSC runs of the commercial thermosets yielded exothermic reactions during cure while the thermoplastics showed endothermic reactions identified as evaporation. The starting and ending cure temperatures show the cure schedule of each material.

It was initially assumed that observed drifts in electrical properties were evidence of incomplete thermal processing, despite having followed manufacturers' recommendations precisely. However, no evidence has been found for additional higher cure temperatures, for example, and explanations for drift remain speculative.

IX. PERCOLATION EFFECTS

The metal particles in the commercial products are irregularly shaped flakes of distributed dimensions. Such structures are not amenable to percolation modeling, so materials with more idealized structures have been fabricated in the laboratory, to relate electrical properties to structure and percolation theory.

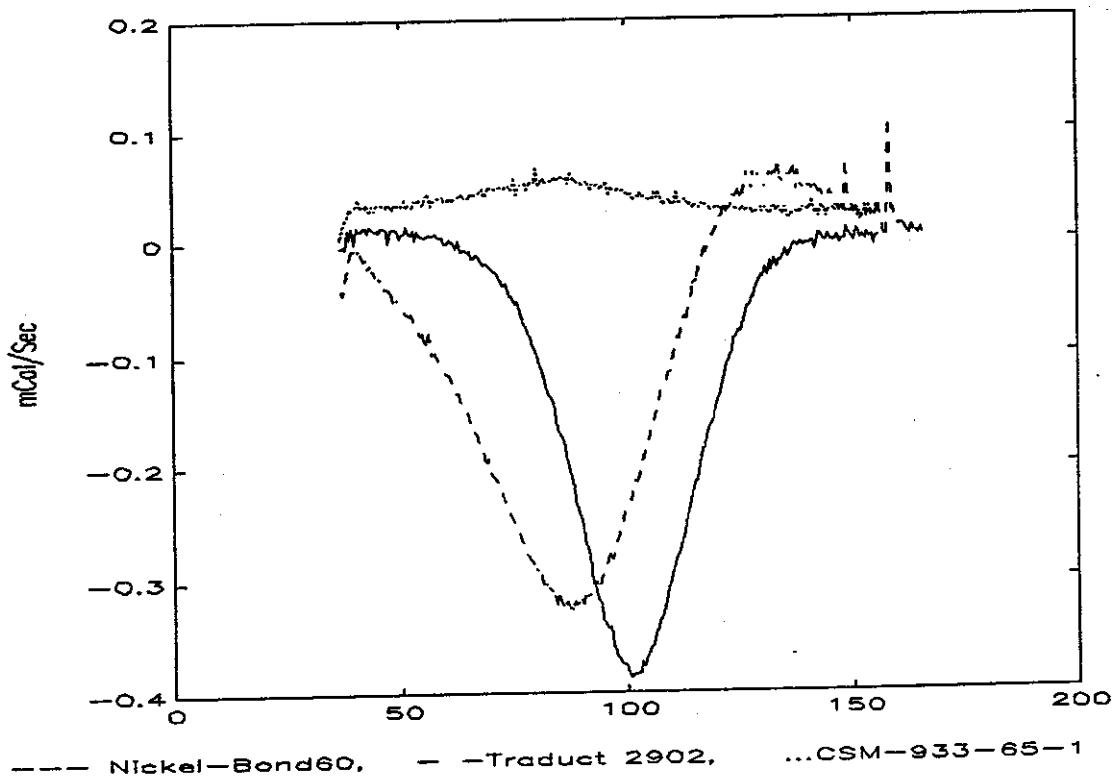


Fig. 10. DSC results of the curing conductive adhesives.

This section describes some preliminary experiments on the resistances of some laboratory fabricated ECA's. Percolation theory predicts a rapid decrease in resistance for many ECA's at the critical metal filler volume concentration V_c of about 20%–30% [20].

Specimen Preparation

For this experiment, a thermosetting epoxy (EPON-828, Shell), a curing agent (TETA, Pacific Anchor Chemicals), and spherical nickel particles (average diameter of 5 μm) were used to make six different samples of filler concentrations 20%, 30%, 40%, 50%, 60%, and 70%. Two 1 \times 1 cm aluminum plates were adhered to each side of the 0.3-cm-thick specimens to form the measurement contacts.

X. RESULTS

DC conductivity and impedance versus frequency measurements were carried out for each sample. These procedures were repeated with multiple samples to verify consistent results.

DC Conductivity: Fig. 11 shows the resistivity variation with composition as measured with a Keithley 169 DMM and 617 electrometer.

Frequency Effects: The impedance change with respect to frequency variation ranging from 100 Hz to 10 MHz is portrayed in Fig. 12. (The HP4194A was again used for the measurement.)

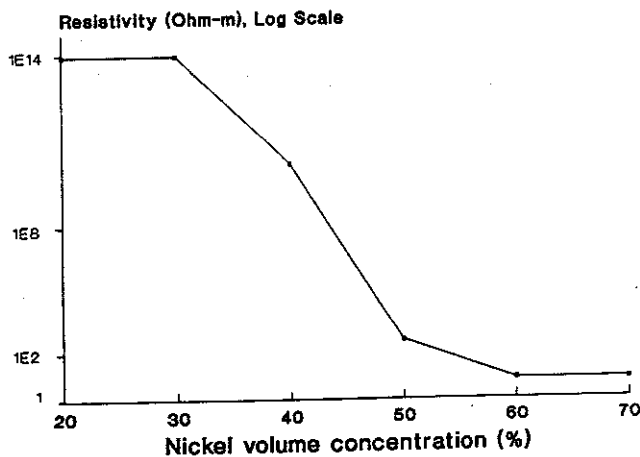


Fig. 11. Resistivity versus nickel volume concentration of ECA.

XI. DISCUSSION

For these particular nickel-sphere filled adhesives, the critical concentration V_c (for the onset of significant conduction) occurred at about 50%–60% nickel volume concentrations. Although this is very different from the theoretical, Fig. 11 displays the expected general trend.

For the frequency effect, no significant changes were seen for adhesives with nickel concentrations of more than 50% by volume, i.e., beyond V_c . (This behavior is identical to that of many commercial ECA's which are filled with "flake" metal particles. The absence of skin effect observations is due to the relatively high resistivity of nickel in comparison with silver.) Impedance decreases are observed as the frequency is

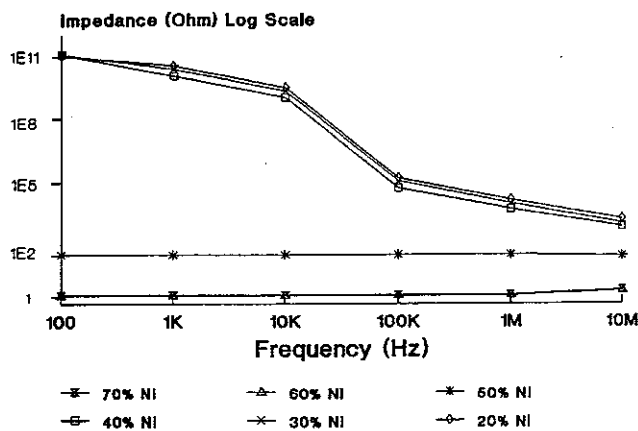


Fig. 12. Impedance versus frequency for nickel-filled ECA's.

increased for less than 50% concentrations, corresponding to the expected effects of interparticulate capacitances. Therefore, capacitive effects do exist below the percolation threshold.

Throughout these experiments, there were two interesting phenomena observed.

1. When sudden pressure and heat are applied to the contacts (e.g., about 160°C with a soldering iron), the resistance quickly drops to around 1 Ω for the 50% filled specimen, i.e., over two orders of magnitude. The detail of the mechanism is unclear, but the system's conductivity is definitely enhanced.
2. No conduction was observed for any sample when point contact probes were used for the measurements without the aluminum plates. This is consistent with Monte Carlo percolation simulations for good conduction [21], where the distance between the contacts should be kept small, with the area of the electrode contacts large.

XII. CONCLUSION

ECA resistances are primarily due to bulk metal conduction, with negligible particle contact effects. The high frequency measurement data can be explained by skin effect, which is a fundamental and unavoidable phenomenon for a good conductor, but predictable.

In comparisons of two competing technologies, it must be remembered that solder is a mature technology with extensive research conducted over decades. The ECA technology is relatively new, with comparatively little data available yet. Before one can reach informed conclusions about the viability of solder replacement, more information about conductive adhesives is required. With the development of new materials, reliability tests of conductive adhesives, and especially with improvements in the fundamental understanding of these materials, that stage will be reached step by step.

XIII. ACKNOWLEDGMENT

We would like to thank H. Eichelberger for his generous help with the SEM and EDS analyses. Special thanks are due to S. Szelag from Fisons Instrument for the EDS analysis, E. J. Cotts for allowing us to use the D.S.C., and W. Blose for his

help and suggestions. We would also like to thank Ablestik, Emerson & Cuming, and Tra-Con for donating samples for our experiments.

REFERENCES

- [1] P. B. Jana, S. Chaudhuri, A. K. Pal, and S. K. De, "Electrical conductivity of short carbon fiber-reinforced carbon polychloroprene rubber and mechanism of conduction," *Polymer Eng. Sci.*, vol. 32, pp. 448-456, Mar. 1992.
- [2] A. Malliaris and D. T. Turner, "Influence of particle size on the electrical resistivity of compacted mixtures of polymers and metallic powders," *J. Appl. Phys.*, vol. 42, pp. 614-618, 1971.
- [3] T. E. Hughes, "Particle size compaction and its effect on conductive coatings, adhesives, and inks," *Circuit Expo '84 Proc.*, 1984, pp. 76-78.
- [4] J. C. Bolger and S. L. Morano, "Conductive adhesives: How and why they work," *Adhesives Age*, pp. 17-20, June 1984.
- [5] A. Burkhart, H. Yoshigahara, Y. Sagami, and T. Yamazaki, "Conductive polymeric adhesives solve SMD assembly problems," *Adhesives Age*, pp. 36-39, Oct. 1990.
- [6] H. A. King, "Polymer based solder alternatives," *Surface Mount Technol.*, pp. 46-49, Aug. 1988.
- [7] B. T. Alpert and A. J. Schoenberg, "Conductive adhesives as a soldering alternative," *Electron. Packaging Production*, pp. 130-132, Nov. 1991.
- [8] R. H. Estes and F. W. Kulcsza, "Surface mount technology—The epoxy alternative," Epoxy Technology, Inc., 14 Fortune Drive, Billerica, MA 01821.
- [9] R. Batson, "The next wave of SMT adhesives," *Circuits Manuf.*, pp. 49-57, Sept. 1990.
- [10] R. Pound, "Conductive epoxy is tested for SMT solder replacement," *Electron. Packaging Production*, pp. 86-90, Feb. 1985.
- [11] L. Taylor, *Metals Handbook*. American Society for Metals, May 1952, pp. 1110-1111.
- [12] S. Ramo, J. R. Whinnery, and T. V. Duzer, *Fields and Waves in Communication Electronics*. New York: Wiley, 1986, pp. 146-153.
- [13] F. W. Grover, *Inductance Calculations: Working Formulas Tables*. General Publishing Company, Ltd., 1946, pp. 261-264.
- [14] A. Duetsch, G. V. Kopsay, V. A. Ranieri, J. K. Cataldo, E. A. Galligan, W. S. Graham, R. P. McGouey, S. L. Nunes, J. R. Paraszczak, J. J. Ritsko, R. J. Serino, D. Y. Shin, and J. S. Wilczynski, "High-speed signal propagation on lossy transmission lines," *IBM J. Res. Develop.*, vol. 34, pp. 601-615, July 1990.
- [15] H. Kim, "Impedance measurement of conductive adhesives," Master's thesis, Binghamton University, Aug. 1992, pp. 43-51.
- [16] S. K. Bhattacharya, *Metal Filled Polymers*. Marcel Dekker, 1986, pp. 27-28.
- [17] A. M. Lyons, "Electrically conductive adhesives: Effect of particle composition and size distribution," *Polymer Eng. Sci.*, vol. 31, pp. 445-450, Mar. 1991.
- [18] R. H. Estes, "The effect of porosity on mechanical, electrical and the thermal characteristics of conductive die-attach adhesives," *Solid State Technol.*, vol. 8, p. 191, 1984.
- [19] B. E. Springett, "Conductivity of a system of metallic particles dispersed in an insulating medium," *J. Appl. Phys.*, vol. 44, pp. 2925-2926, 1973.
- [20] F. T. de Araujo and H. M. Rosenberg, "Switching behavior and dc electrical conductivity of epoxy-resin/metal-powder composites," *J. Phys. D: Appl. Phys.*, vol. 9, pp. 1025-1030, 1976.
- [21] G. R. Ruschau, S. Yoshikawa, and R. E. Newnham, "Percolation constraints in the use of conductor-filled polymers for interconnections," in *Proc. 42nd IEEE Electronic Components and Technology Conf.*, May 18-20, 1992, pp. 481-486.



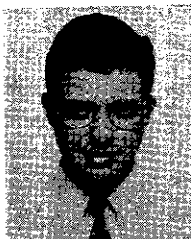
Li Li received the B.S. and M.S. degrees in materials science and engineering from the University of Science and Technology, Beijing, China.

She was employed by Nanya Technology Co., Shenzhen, China, where she worked on processing techniques for conductive ITO thin films. She is currently a candidate for the Ph.D. degree, conducting research in conductive adhesives in the Department of Electrical Engineering at Binghamton University.



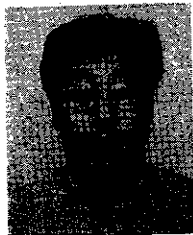
Christine Lizzul received both the B.S.E.E. and M.S.E.E. degrees from Binghamton University. She is currently a candidate for the Ph.D. degree at North Carolina State University.

Ms. Lizzul is a member of Tau Beta Pi and was a cofounder of the local chapter of the Society of Women Engineers. She has been nominated for campus honors recognizing both SWE service and academic achievement.

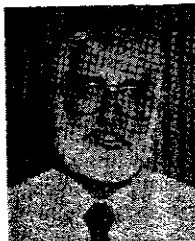


Isaac Sacolick received the B.S.E.E. degree from Binghamton University and is pursuing graduate studies at the University of Arizona.

Mr. Sacolick is president of Eta Kappa Nu, a member of Tau Beta Pi, and was recognized at Binghamton for outstanding service to his department.



Hansoo Kim received the B.S.E.E. degree from Case Western Reserve University and the M.S.E.E. degree from Binghamton University. He is currently enrolled in the Ph.D. program in the Department of Electrical Engineering at the University of Pittsburgh.



James E. Morris (S'69-M'70-SM'82) is Chairman of the Department of Electrical Engineering, Binghamton University. He was the first Director of Binghamton's Institute for Research in Electronics Packaging, which became the Integrated Electronic Engineering Center jointly funded by local industry, New York State, and the National Science Foundation. The Center was recently designated as a New York State Center for Advanced Technology.